Materials Research Proceedings **26** (2023) 461-466 https://doi.org/10.21741/9781644902431-75

Experimental characterisation and numerical modelling of axially loaded wire rope isolators

Davide Pellecchia[1, a *], Nicolò Vaiana[1, b], Salvatore Sessa[1, c], Francesco Marmo[1, d] and Luciano Rosati[1, e]

[1]Department of Structures for Engineering and Architecture, University of Naples Federico II, Naples, Italy

[a]davide.pellecchia@unina.it, [b]nicolo.vaiana@unina.it, [c]salvatore.sessa2@unina.it, [d]f.marmo@unina.it, [e]rosati@unina.it

Keywords: Wire Rope Isolators, Experimental Tests, Hysteretic Model

Abstract. We present the main outcomes of a recent experimental activity denoted to studying the dynamic behaviour of Wire Rope Isolators loaded along the axial direction. The experimental activity has been carried out at the laboratory of the Department of Structures for Engineering and Architecture of the University of Naples Federico II (Italy). Furthermore, a new hysteretic model derived from a recently developed class of asymmetric hysteretic models is illustrated. The main advantages of the proposed model with respect to the classical ones, typically having a differential nature, are: 1) the output variable is computed in closed-form, i.e. without numerically solving a differential equation; 2) the proposed model is based on two different sets of parameters that allows one to independently model the loading and unloading curves. Specifically, a close matching between the experimental asymmetric loop and the numerically one has been obtained.

Introduction

Wire Rope Isolators (WRIs) are widely used in controlling both vibration and shock in order to protect sensitive equipment in the areas of aerospace and mechanical engineering [1] as well as for seismic protection of buildings [2] and their contents/equipment [3]. These devices have also been used to reduce the seismic vibration in protecting high voltage ceramic circuit breakers [4] and to protect the two Riace bronzes towards vertical components of seismic ground motions [5,6].

The excellent damping properties of such a device are due to the sliding friction developed between strands and wires that allows one to dissipate a large amount of energy. In addition, the WRIs behaviour depends on the device's geometrical characteristics, e.g. the device length (l), width (w), height (h) and the wire rope diameter (ϕ).

The WRIs force-displacement curve is affected by geometrical and mechanical non-linearities resulting in a complex shape of hysteretic nature that depends on the direction along which the devices are loaded, i.e., typically, the shear, roll and axial directions [7], see, e.g., Fig. 1. As a matter of fact, the hysteretic loop is symmetric in both shear and roll directions, while along the axial direction is asymmetric, showing a remarkable difference between tension and compression behaviour [8].

The complex WRI behaviour is typically predicted by using hysteretic models of differential nature [9,10] including the well-known Bouc-Wen model [11,12]. These kinds of models show some issues, such as: 1) the evaluation of the output variable is performed by numerically solving a differential equation; 2) generally, the models' parameters have a not clear physically meaning; 3) the loading and unloading branches in the force-displacement curve are coupled; 4) they must be suitably modified to reproduce specific force-displacement curves such as asymmetric loops.

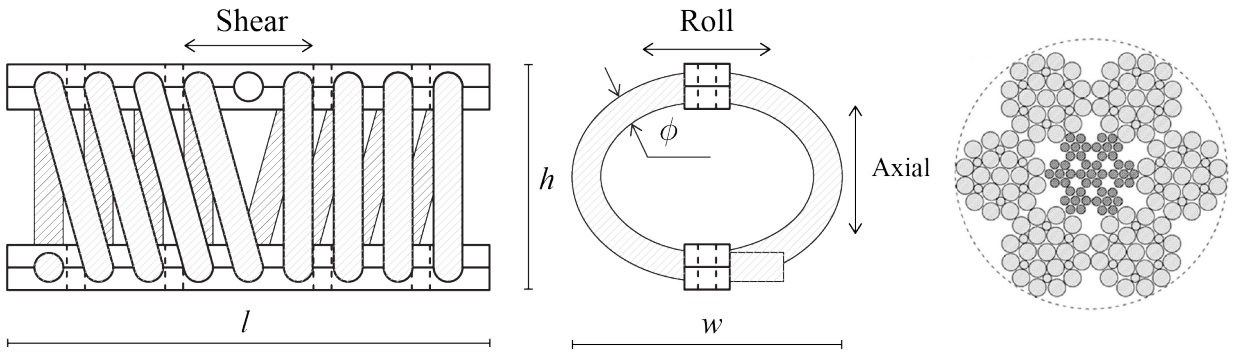

(a) Front view *(b) Transverse view* *(c) Cable's cross-section*

Figure 1 Geometrical characteristics of WRIs and load directions.

Being interested to characterise the dynamic behaviour of WRIs along the axial direction, we illustrate some preliminary results obtained for the PWHS16040 device manufactured by Powerflex S.r.l (Limatola, Italy) during an experimental campaign conducted at the laboratory of the Department of Structures for Engineering and Architecture of the University of Naples Federico II (Italy). Finally, the mathematical characterisation of such a behaviour is shown by adopting a new hysteretic model.

Experimental activity and results

The preliminary results of the experimental campaign carried out on the WRI PWHS16040 loaded along the axial direction in both small and large displacements regimes are described in this Section. Specifically, the force-displacement (*f*-*u*) curves are compared, aiming to investigate the dynamic behaviour of the above-mentioned device by studying the influence of the displacement amplitude and frequency of a sinusoidal displacement input as well as of the axial preload and of the wire rope diameter.

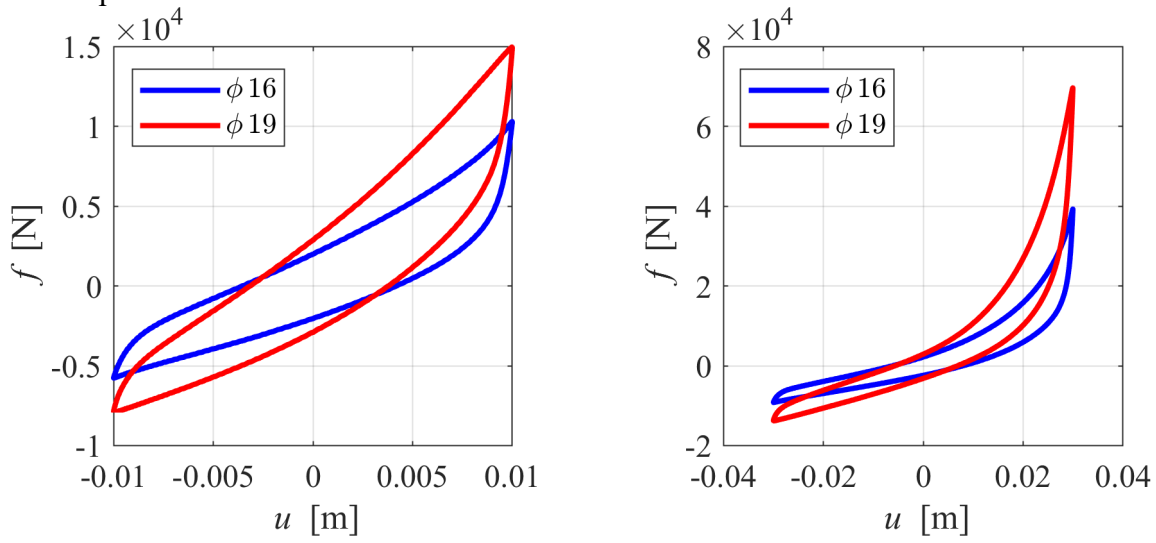

(a) Displacement amplitude ± 0.01 meters *(b) Displacement amplitude ± 0.03 meters*

Figure 2 Hysteresis loops exhibited by two PWHS16040 devices characterised by two different diameters of the wire rope.

Fig. 2 shows the hysteresis loops obtained for two PWHS16040 devices equipped with two different wire ropes having diameters equal to 16 mm (blue curves) and 19 mm (red curves), and by applying, in absence of axial preload, sinusoidal displacements having a frequency of 0.1 Hz and amplitudes equal to 10 mm (left) and 30 mm (right). One can observe that the use of a large

Materials Research Proceedings **26** (2023) 461-466 https://doi.org/10.21741/9781644902431-75

wire rope diameter provides a clockwise rotation of the hysteresis loops both in small and large displacements.

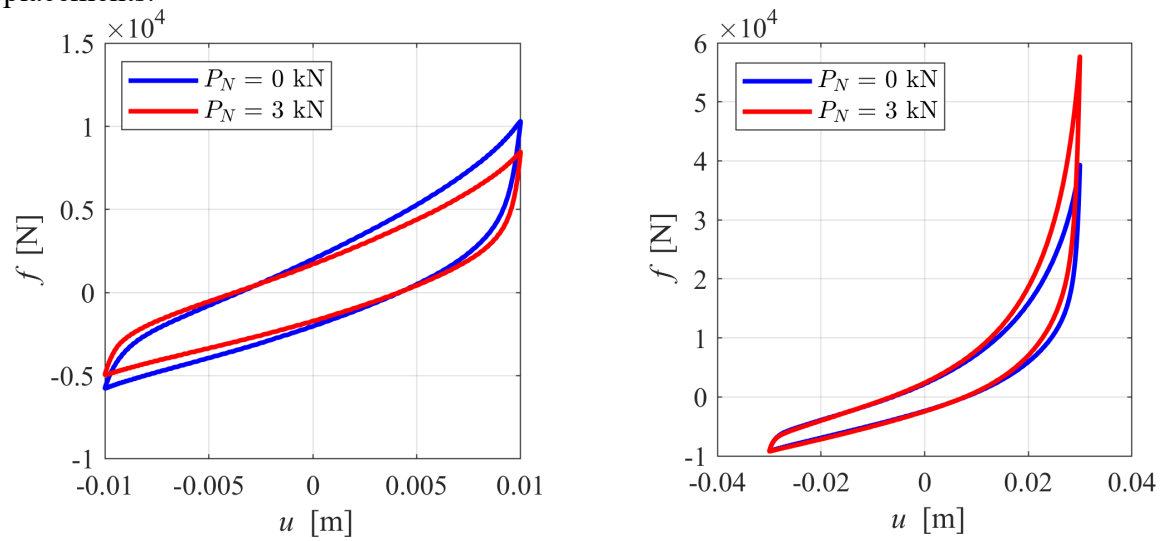

(a) Displacement amplitude ± 0.01 meters *(b) Displacement amplitude ± 0.03 meters*

Figure 3 Hysteresis loops obtained in absence of axial preload from cyclic tests characterised by a frequency of 0.1 Hz.

Hence, by increasing the wire rope diameters, the tangent stiffnesses in the state of tension and compression increase. In addition, a larger amount of dissipated energy, which is represented by the area enclosed in the hysteresis loop, is shown using a large wire rope diameter, mainly in the large displacements range.

The hysteresis loops of the WRI PWHS16040 are plotted in Fig. 3 as a function of the axial preload by applying sinusoidal displacements having a frequency of 0.1 Hz and amplitudes equal to 10 mm (left) and 30 mm (right). Notably, two values of axial preload are considered, namely 0 (blue curve) and 3 kN (red curves). The hysteresis loop exhibits a clockwise rotation, without changing its area, when the displacement amplitude is equal to 10 mm and the axial preload increases (see Fig.3(a)). On the other hand, in the range of large displacements (Fig. 3(b)), a stiffening behaviour in the state of tension is displayed when the axial preload is increased, whereas the tangent stiffness variation in the state of compression is negligible.

Fig. 4 shows the hysteresis loops obtained for the WRI PWHS16040 device, in absence of axial preload, when subjected to a sinusoidal displacement having displacements amplitude equal to 10 mm and 30 mm, see, e.g., Fig. 4(a) and (b), respectively, and increasing frequency. By increasing the input frequency, a pronounced hardening behaviour in the state of tension is shown for large displacements, while the change of the tangent stiffness in the state of compression remains negligible, see Fig. 4(b). In contrast, the frequency effect on the tested WRI is much lower at small displacements, see Fig. 4(a).

Experimental validation

In this Section, we derive a specific hysteretic model from a more general class of models [13]; subsequently the new model is validated by comparing the experimental hysteresis loops of the PWHS16040 device with the simulated one.

The general idea of the class of models consists of splitting the loop into four distinct curves that describe two phases, namely the generic loading and unloading phases in which the generalised velocity is, respectively, greater and smaller than zero.

Materials Research Proceedings **26** (2023) 461-466 https://doi.org/10.21741/9781644902431-75

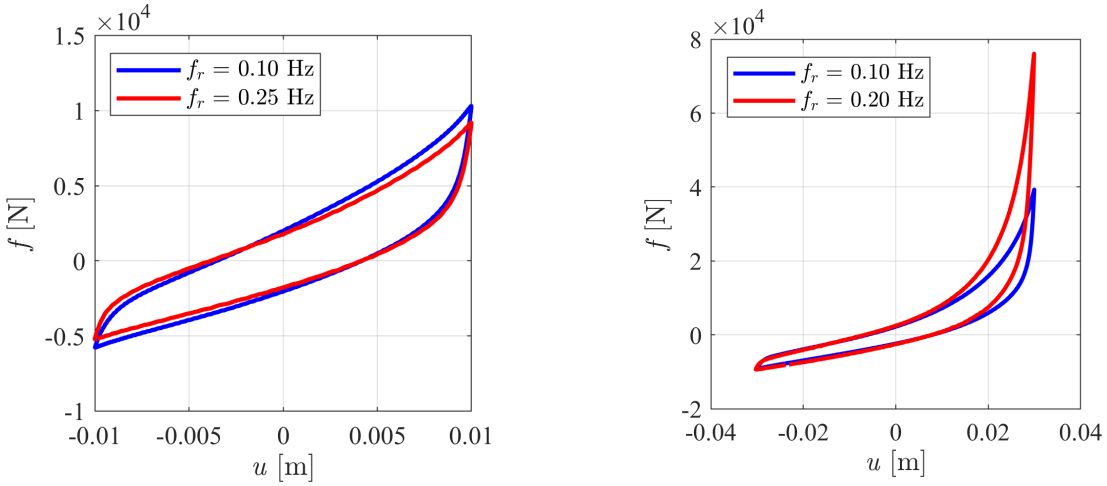

(a) Displacement amplitude ± 0.01 meters *(b) Displacement amplitude ± 0.03 meters*

Figure 4 Hysteresis loops obtained in absence of axial preload from cyclic tests characterised by increasing values of frequency f_r.

Notably, the generic loading phase is described by the loading and upper limiting curves denoted as c^+ and c_u, respectively; whereas the generic unloading phase is defined by the unloading and lower limiting curves referred to, respectively, as c^- and c_l, see, e.g., Fig. 5.

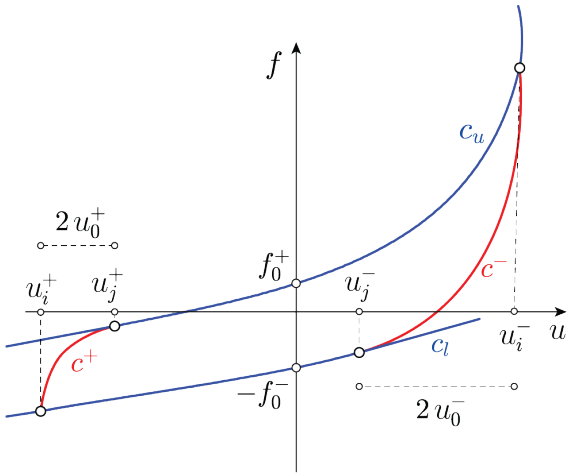

Figure 5 The four curves able to simulate the dynamic behaviour of WRIs.

The experimental validation is carried out by taking into account a hysteretic model belonging to the above-mentioned class. Specifically, the proposed model corresponds to a simplified version of the recently proposed Vaiana-Rosati model (VRM) [14] in which only hysteresis loops characterised by upper and lower limiting curves with no inflexion points are modelled.

Due to space limitations we just report the mathematical expressions of the functions describing the curves relating force *f* and displacement *u* along the axial direction

$$\begin{aligned} c_u(u) &= \beta_1^+ e^{\beta_2^+ u} - \beta_1^+ + k_b^+ u + f_0^+, \\ c_l(u) &= \beta_1^- e^{\beta_2^- u} - \beta_1^- + k_b^- u - f_0^-, \end{aligned} \tag{1}$$

whereas the loading and unloading limiting curves

$$\begin{aligned} c^+(u,u_j^+) &= \beta_1^+ e^{\beta_2^+ u} - \beta_1^+ + k_b^+ u + f_0^+ - \frac{1}{\alpha^+}\left[e^{-\alpha^+\left(+u-u_j^+ +\overline{u}^+\right)} - e^{-\alpha^+ \overline{u}^+}\right], \\ c^-(u,u_j^-) &= \beta_1^- e^{\beta_2^- u} - \beta_1^- + k_b^- u - f_0^- + \frac{1}{\alpha^-}\left[e^{-\alpha^-\left(-u+u_j^- +\overline{u}^-\right)} - e^{-\alpha^- \overline{u}^-}\right]. \end{aligned} \tag{2}$$

The quantities $k_b^+, \alpha^+, \beta_1^+, \beta_2^+, f_0^+ (k_b^-, \alpha^-, \beta_1^-, \beta_2^-, f_0^-)$ represent the constitutive model parameters to be identified, whereas $\bar{d}^+, d_0^+ (\bar{d}^-, d_0^-)$ can be expressed as a function of the above-mentioned parameters. The quantities u_j^+ and u_j^- are illustrated in Fig. 5 and can be evaluated as a function of the coordinates of a generic initial point that lies on the upper or lower limiting curve. The relevant expressions and their mechanical significance are omitted for brevity.

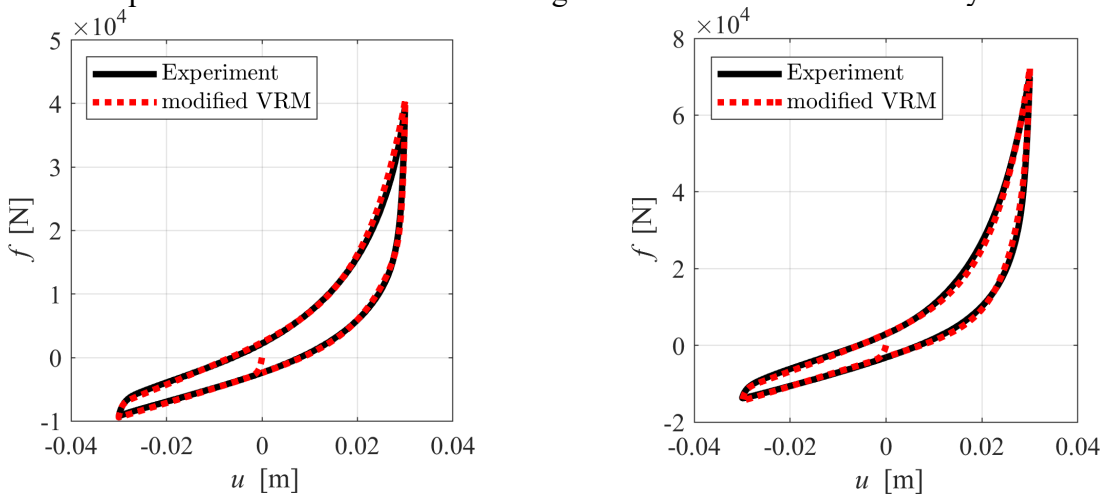

(a) Wire rope diameter ϕ 16 *(b) Wire rope diameter ϕ 19*

Figure 6 Experimental hysteresis loops vs. simulated ones obtained by using the model parameters listed in Tab. 1.

Fig. 6 compares the experimental and numerical hysteresis loops obtained for the PWHS16040 device by applying, in absence of preload, a sinusoidal displacement input having a frequency of 0.1 Hz and an amplitude of 0.03 m. Specifically, the validation of the modified VRM model has been carried out by assuming two wire ropes having different diameters, i.e. 16 mm (Fig. 6(a)) and 19 mm (Fig. 6(b)) and the constitutive model parameters listed in Tab. 1.

The numerical hysteresis loops obtained by means of the proposed hysteretic model are depicted by the dotted red lines, whereas the solid black lines represent hysteresis loops obtained by experimental tests. Such a comparison shows an excellent match between the two hysteresis loops, demonstrating that the proposed hysteretic model can satisfactorily predict the WRI's dynamic response.

Table 1 Model parameters used for reproducing hysteresis loops in Fig. 6.

ϕ [mm]	$\mathrm{sgn}(\dot{u})$	k_b [N m^{-1}]	f_0 [N]	α [m^{-1}]	β_1 [N]	β_2 [m^{-1}]
16	+	300 000	2 400	1 800	750	125
	-	225 000	2 400	1 800	250	140
19	+	450 000	3 015	1 500	850	140
	-	380 000	3 015	1 500	60	220

Conclusions

We have presented some preliminary results of an experimental campaign, on the PWHS16040 device manufactured by Powerflex S.r.l. loaded along the axial direction, that has been carried out at the laboratory of the Department of Structures for Engineering and Architecture of the University of Naples Federico II (Italy). Specifically, aim of experimental campaign was to investigate the dynamic behaviour of the device by studying the influence of the amplitude and frequency of a sinusoidal displacement input as well as of the axial preload and of the wire rope diameter.

The experimental outcomes have shown that the effects of the frequency input and the axial preload do not significantly change the WRI dynamic behaviour in the field of small displacements. On the contrary, a stiffening behaviour in the state of tension has been shown in the field of large displacements.

Finally, in order to predict the WRI dynamic behaviour along the axial direction, a new hysteretic model has been proposed. Such a model has been calibrated and validated by comparing the experimental hysteresis loops with the numerically simulated ones.

References

[1] M.L. Tinker, M.A. Cutchins, Damping phenomena in a wire rope vibration isolation system, J. Sound and Vib. 157 (1992) 7-18. https://doi.org/10.1016/0022-460X(92)90564-E

[2] M. Spizzuoco, V. Quaglini, A. Calabrese, G. Serino, C. Zambrano, Study of wire rope devices for improving the re-centering capability of base isolated buildings, Struct. Control. Health. 24(6) (2017) e1928. https://doi.org/10.1002/stc.1928

[3] G.F. Demetriades, M.C. Constantinou, A.M. Reinhorn, Study of wire rope systems for seismic protection of equipment in buildings, Eng. Struct. 15 (1993) 321-334. https://doi.org/10.1016/0141-0296(93)90036-4

[4] S. Alessandri, R. Giannini, F. Paolacci, M. Malena, Seismic retrofitting of an HV circuit breaker using base isolation with wire ropes. part 1: Preliminary tests and analyses, Eng. Struct. 98 (2015) 251-262. https://doi.org/10.1016/j.engstruct.2015.03.032

[5] G. De Canio, Marble devices for the base isolation of the two bronzes of Riace: a proposal for the David of Michelangelo, P. WCEE (2012).

[6] D. Pellecchia, S. Lo Feudo, N. Vaiana, J.-L. Dion, L. Rosati, A procedure to model and design elastomeric-based isolation systems for the seismic protection of rocking art objects, Comput. Aided Civ. Inf. (2022) 1-18.

[7] N. Vaiana, M. Spizzuoco, G. Serino, Wire rope isolators for seismically base-isolated lightweight structures: Experimental characterization and mathematical modeling, Eng. Struct. 140 (2017) 498-514. https://doi.org/10.1016/j.engstruct.2017.02.057

[8] F. Foti, J. Galeazzi, L. Martinelli, On the modelling of the Hysteretic Behaviour of Wire Rope Isolators, P. XXIV AIMETA (2020) 1535–1542. https://doi.org/10.1007/978-3-030-41057-5_124

[9] S. Rashidi, S. Ziaei-Rad, Experimental and numerical vibration analysis of wire rope isolators under quasi-static and dynamic loadings, Eng. Struct. 148 (2017) 328-339. https://doi.org/10.1016/j.engstruct.2017.06.061

[10] A. Salvatore, B. Carboni, L.Q. Chen, W. Lacarbonara, Nonlinear dynamic response of a wire rope isolator: Experiment, identification and validation, Eng. Struct. 238 (2021) 112121. https://doi.org/10.1016/j.engstruct.2021.112121

[11] R. Bouc, Modèle mathématique d'hystérésis, Acustica 24 (1) (1971) 16-25.

[12] Y. K. Wen, Method for random vibration of hysteretic systems, J. Eng. Mech. Div. 102 (2) (1976) 249-263. https://doi.org/10.1061/JMCEA3.0002106

[13] N. Vaiana, S. Sessa, L. Rosati, A generalized class of uniaxial rate-independent models for simulating asymmetric mechanical hysteresis phenomena, Mech. Syst. Signal Pr. 146 (2021) 106984. https://doi.org/10.1016/j.ymssp.2020.106984

[14] N. Vaiana, L. Rosati, Classification and Modeling of Uniaxial Rate-Independent Hysteresis Phenomena: Some Preliminary Results, P. XXV AIMETA (2022).